DTU Library

Improving the All-Optical Response of SOAs Using a Modulated Holding Signal

Bischoff, Svend; Nielsen, Mads Lønstrup; Mørk, Jesper

[Link back to DTU Orbit](#)

Improving the All-Optical Response of SOAs Using a Modulated Holding Signal

S. Bischoff, M. L. Nielsen, and J. Mørk

Abstract—A method for increasing the all-optical modulation bandwidth of semiconductor optical amplifiers (SOAs) by use of a cross-gain-modulated (XGM) holding signal is suggested and analyzed. The bandwidth improvement is numerically demonstrated by studying wavelength conversion in an SOA-based Mach-Zehnder interferometer (MZI) at 160 and 40 Gb/s. The new scheme is predicted to improve the extinction ratio and the minimum mark output power, as well as to reduce the amplitude jitter of the wavelength converted signal.

Index Terms—Interferometer, optical signal processing, patterning, semiconductor optical amplifier (SOA), wavelength conversion.

I. INTRODUCTION

ALL-OPTICAL signal processing is expected to be a key functionality in telecommunication networks with transmission capabilities beyond 100 Gb/s. Devices based on semiconductor optical amplifiers (SOAs) for all-optical demultiplexing, wavelength conversion, regeneration, optical logic, etc. have already been intensively investigated [1]–[4]. Error-free demultiplexing of a 252 Gb/s signal to 10.5 Gb/s has been experimentally demonstrated in an SOA based symmetric Mach-Zehnder switch [1], and error-free wavelength conversion of a 168 Gb/s signal has been achieved in a delayed interference semiconductor wavelength converter (DISC) [2]. In the latter case, the power penalty for observing a bit error rate (BER) of 10^{-9} was as high as 6 dB, and the pseudorandom bit sequence (PRBS) length was limited to $2^7 - 1$. These limitations are attributed to inherent patterning effects associated with the gain recovery process in an SOA.

Allthough error-free wavelength conversion has been experimentally demonstrated at 168 Gb/s [2], the high amplitude jitter of the converted signal impedes the use of this signal for further transmission and possible use in all-optical signal processing configurations. In the conventional wavelength conversion scheme, the data signal and a CW signal, onto which the data information is transferred, are injected into an SOA (cross-gain modulation—XGM) or a Mach–Zehnder interferometer (MZI) (cross-phase modulation—XPM). It is well known, that stimulated emission due to the CW signal reduces the effective gain recovery time, thereby increasing the bandwidth of the device. This effect has been utilized to further
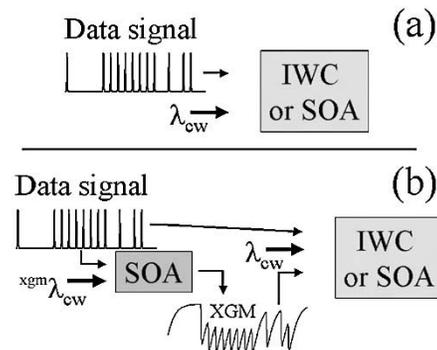
Fig. 1. Schematic of wavelength conversion by XPM (XGM) in an interferometric wavelength converter (IWC) or SOA without (a) and with (b) a modulated holding signal. The modulated holding signal could be generated by XGM in an SOA as indicated (b).

improve the modulation bandwidth by the injection of a third CW signal, denoted a holding beam [3]. This is schematically shown in Fig. 1(a).

In this paper a novel scheme is proposed, which increases the modulation bandwidth of SOAs used for all-optical signal processing by applying a time-varying holding signal, which is partly inverted with respect to the data signal. This modulated holding signal can conveniently be generated in an SOA by XGM, as depicted in Fig. 1(b), or by the use of an SOA based interferometer. The XGM scheme requires an extra SOA and an additional signal (the XGM holding signal), but the additional SOA can in principle be monolithically integrated with the switching device. The idea of using a holding signal, which is an inverted and low-pass filtered version of the data signal, is basically to temporally equalize the total power injected into the SOA, thereby reducing the degree of patterning.

The temporal characteristics of the modulated holding beam are important. The optical response of a wavelength converter relying on XGM would obviously deteriorate if the holding signal instantaneously made up for the changes in the data signal. On the contrary, slower changes of the modulated holding signal can mitigate pattern effects by equalizing the average power level injected into the SOA for, say, a long string of marks or a long string of spaces. The optimum bandwidth of the modulated holding signal depends on the all-optical modulation technique being used. In case of four wave mixing (FWM) in an SOA, the use of a perfectly inverted signal would ideally make it possible to keep the optical power constant, since, in this case, the modulated holding signal can be orthogonally polarized with respect to the data signal and the signal onto which the data information is transferred.

In this paper, we specifically investigate the influence of a modulated holding signal on the performance of a MZI operating in differential mode. In this scheme [6], the data signal and a delayed version of it are injected into the two arms of an MZI, cf. Fig. 2. The transmission of the CW signal through the interferometer is governed by the phase-difference between the two SOAs, thus reducing the degree of patterning compared to a scheme where only one interferometer arm is modulated, or an XGM scheme. However, as noted earlier, long-term patterning effects may still prevail, as indicated by the experimental problem in converting long PRBS sequences [2]. By injecting a modulated holding signal into both arms simultaneously, cf. Fig. 2, one may thus counterbalance the SOA saturation without significantly changing the phase difference. In this way one limits the degree of power fluctuations, and thus saturation, of the SOA.

The paper is organized as follows. First, we briefly summarize the large-signal model employed for the simulations. Next, the scheme is investigated for wavelength conversion at 160 Gb/s. A separate section is dedicated to the investigation of the scheme at a moderate speed of 40 Gb/s, where both the inverted and noninverted output are simultaneously optimized. The details of the modulated holding signal are investigated in this case.

II. MODEL

The large signal model used to investigate the wavelength conversion scheme has been described in [6]. The equations describing field propagation are as follows:

$$\pm \frac{dE^{\pm}}{dz} + \frac{1}{v_g}\frac{dE^{\pm}}{dt}$$
$$= \frac{1}{2}(\Gamma g - \alpha_{\text{int}})E^{\pm} + \frac{i}{2}(\alpha_N \Gamma \Delta g_N + \alpha_T \Gamma \Delta g_T)E^{\pm}$$
$$+ (\text{in}_{\text{TPA}} - \beta_{\text{TPA}})SE^{\pm} - i\frac{\Gamma}{2}\frac{dg}{d\omega}\frac{dE^{\pm}}{dt}$$
$$+ \left(\frac{i}{2}\beta_2 - \frac{\Gamma}{4}\frac{d^2g}{d\omega^2}\right)\frac{d^2E^{\pm}}{dt^2}. \tag{1}$$

The normalization of the electrical field amplitude is chosen such that the photon density is $S = |E^+|^2 + |E^-|^2$, where E^+ and E^- are the right and left propagating fields, respectively.

The symbols z and t represent the space and time coordinates. Other parameters are v_g as the group velocity, Γ is the optical confinement factor, α_{int} is internal loss, n_{TPA} and β_{TPA} are Kerr and two photon absorption (TPA) coefficients, β_2 is group velocity dispersion, $dg/d\omega$ and $d^2g/d\omega^2$ are gain dispersion, α_N and α_T represents linewidth enhancement factors accounting for self-phase modulation due to changes in the carrier density and the carrier temperature, respectively.

The dynamical gain g of the SOA is determined by a set of rate equations derived from semi-classical density matrix equations [7]–[9], where the carrier distribution functions are relaxing toward quasi-Fermi-Dirac distributions by carrier-carrier and carrier-phonon scattering with characteristic (phenomenolog-
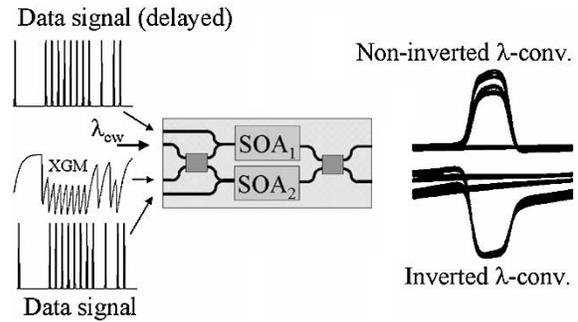

Fig. 2. Schematic of wavelength conversion in a MZI using a modulated holding signal. The modulated holding signal is simultaneously injected into both SOAs of the MZI. The eye diagrams for both inverted and noninverted wavelength conversion are shown at the right-hand side (RHS).

ical) time constants. The rate equations for the total carrier density N, energy density U_x, and local carrier density n_x are

$$\frac{dN}{dt} = \frac{I}{eV} - v_g\sum_\lambda g_\lambda S_\lambda$$
$$- A_{\text{nr}}N - BN^2 - C_{\text{nr}}N^3 \tag{2}$$
$$\frac{dU_x}{dt} = -\frac{U_x - U_x^L}{\tau_{h,x}}$$
$$+ \sum_\lambda (\sigma_x N\hbar\omega_0 v_g - E_{x,\lambda,0}g_\lambda)S_\lambda \tag{3}$$
$$\frac{dn_{x,\lambda}}{dt} = -\frac{n_x - \overline{n}_x}{\tau_{1,x}} - v_g g_\lambda S_\lambda \tag{4}$$

where x stands for conduction (c), heavy hole (hh), and light hole band (lh), $(x = c, \text{lh}, \text{hh})$, respectively. Other parameters are I as injection current, e is the electron charge, V as the volume of active area, A_{nr}, B, and C_{nr} are radiative and nonradiative recombination coefficients, U_x^L is carrier energy density at the lattice temperature, $\tau_{h,x}$ represents carrier temperature relaxation time constant, ρ_x is free carrier absorption cross section, $E_{x,0}$ is reference energy, $\overline{n}_x$ is gain determining local carrier density for quasi-equilibrium, an $\tau_{1,x}$ is relaxation time constant for spectral hole burning. The gain g is

$$g_\lambda = a_N(n_{c\text{hh},\lambda} + n_{\text{hh},\lambda} - N_{0\text{hh},\lambda})$$
$$+ a_N\left(n_{c\text{lh},\lambda} + n_{\text{lh},\lambda} - N_{0\text{lh},\lambda}\right) \tag{5}$$
$$a_N = \frac{|d_{\text{cv}}|^2\gamma_2^{-1}\omega_0}{\hbar\epsilon_0 n_e c} \tag{6}$$

where $|d_{\text{cv}}|$ is the dipole-moment, $\gamma_2 = 1/\tau_2$ is the decay rate for the polarization, c is the speed of light in vacuum, n_e is the refractive index, and ϵ_0 is the electric permittivity. The parameter values used in our simulations are given in Table I. The rate equations for carrier density, carrier energy, and local carrier density have been solved by a Runge-Kutta scheme, while field propagation is accounted for by using a modified method-of-lines scheme, where the dispersion terms have been included by using values from the previous time step.

III. WAVELENGTH CONVERSION AT 160 Gb/s

Noninverted wavelength conversion is, in the configuration considered here, accomplished by applying the same bias to

both SOAs, since a $\pi/2$ phase shift is assumed between the output ports of the multi-mode interference couplers. The modulated holding signal in Fig. 2 can be generated by XGM in an additional SOA [see Fig. 1(b)]. The holding signal is, whether CW or modulated, injected into both MZI SOAs simultaneously as shown in Fig. 2, while there is a time-delay between the data signals entering the lower and upper SOA. The wavelengths of the data, converted and holding signal have been set at 1520, 1530, and 1525 nm, respectively. The data signal was generated from a $2^4 - 1$ PRBS signal, where the different 4-bit patterns were cyclically interchanged, resulting in a data sequence with characteristics similar to that of a $2^7 - 1$ PRBS sequence, e.g., with a maximum of eight consecutive marks, mark-space or spaces.

Fig. 3 shows the optical eye diagrams for the wavelength-converted signal and a fraction of the corresponding data and holding signal for wavelength conversion in a MZI with 1 mm long SOAs at 160 Gb/s. The data signal had an average power of 2 dBm and consisted of Gaussian pulses with a full width at half maximum of 2 ps. The differential time delay between the two data signals was set to 3 ps. Fig. 3(a) and (b) are for the case of a strong and a weak CW holding signal, respectively. The amplitude jitter is seen to decrease with increasing CW holding signal power, but at the same time the eye opening is reduced. As mentioned in the introduction, the purpose of a CW holding signal is to reduce the effective carrier lifetime [5]. However, a strong CW holding signal also reduces the carrier density in the SOA, resulting in a reduction of the gain and refractive index changes induced by the data signal. Thus, optimum values for the power levels of the data and CW holding signal exist for a given SOA and bit rate.

The fluctuations in the mark power level (FMPL) (max. mark level/min. mark level) and the extinction ratio (ER) (min. mark level/max. space level) are plotted in Fig. 4 as function of CW holding signal power. The data signal was the same as studied in Fig. 3. As aforementioned, the FMPL decreases with increasing CW holding signal power, while the ER shows an optimum for a CW holding signal power of 1–2 dBm. The optimum value is related to the data signal power. The ER of the converted signal for a holding signal power of more (less) than 1–2 dBm can be improved by increasing (decreasing) the data signal power.

As aforementioned, the simulations have been performed using a data signal corresponding to a PRBS signal of limited word length. The maximum number of 8 consecutive marks or spaces sets a limit to the observed ER and FMPL for a holding signal power below -1 dBm. A longer PRBS signal would result in slightly lower (higher) ER (FMPL), since steady state is not reached for a low holding signal power when converting a sequence of eight consecutive marks. Increasing the CW holding signal power to 2 dBm, or employing modulated holding signals [Fig. 3(c) and (d)], the conversion of eight consecutive marks is shown to be sufficient to estimate the ER and FMPL. This is illustrated in Fig. 5(a), where a fraction of the wavelength converted data signal corresponding to the optical eye in Fig. 3(a) is shown.

The improvement of the signal quality by replacing the CW holding signal with a modulated holding signal is illustrated in Fig. 3(c). The ER is improved and the amplitude fluctuations are

TABLE I
PARAMETER VALUES USED IN THE LARGE SIGNAL SIMULATIONS

| Symbol	Value	unit
m_c conduction band mass	0.0442	m_0
m_{hh} heavy hole mass	0.4356	m_0
m_{lh} light hole mass	0.0564	m_0
m_0 electron mass	$0.911 \cdot 10^{-30}$	kg
$I(500\mu m)$ current	65-75	mA
$I(1000\mu m)$ current	140-150	mA
$V(500\mu m)$ active volume	$1.05 \cdot 10^{-16}$	m^3
$V(1000\mu m)$ active volume	$2.10 \cdot 10^{-16}$	m^3
E_g bandgap	0.79	eV
T_L lattice temperature	300	K
Γ confinement factor	0.45	
α_{int} internal loss	3000	m^{-1}
α_N α-factor	8.0	
α_T α-factor	4.0	
c speed of light	$2.998 \cdot 10^8$	ms^{-1}
v_g group velocity	$0.833 \cdot 10^8$	ms^{-1}
n_e effective index	3.5	
A_{nr} non-radiative recomb.	$1.0 \cdot 10^8$	s^{-1}
B spontaneous recomb.	$9.0 \cdot 10^{-16}$	$m^3 s^{-1}$
C_{nr} Auger recomb.	$0.5 \cdot 10^{-40}$	$m^6 s^{-1}$
σ_c free carrier absorption	$3.5 \cdot 10^{-22}$	m^2
σ_{hh} free carrier absorption	$0 \cdot 10^{-22}$	m^2
σ_{lh} free carrier absorption	$0 \cdot 10^{-22}$	m^2
$\tau_{h,c}$ carrier-phonon scatt.	$0.8 \cdot 10^{-12}$	s
$\tau_{h,hh}$ carrier-phonon scatt.	$0.2 \cdot 10^{-12}$	s
$\tau_{h,lh}$ carrier-phonon scatt.	$0.2 \cdot 10^{-12}$	s
$\tau_{1,c}$ carrier-carrier scatt.	$60 \cdot 10^{-15}$	s
$\tau_{1,hh}$ carrier-carrier scatt.	$40 \cdot 10^{-15}$	s
$\tau_{1,lh}$ carrier-carrier scatt.	$40 \cdot 10^{-15}$	s
τ_2 dephasing time	$40 \cdot 10^{-15}$	s
β_{TPA} two-photon absorption	$0.3 \cdot 10^{-9}$	mW^{-1}
n_{TPA} two-photon absorption	$-8.0 \cdot 10^{-17}$	$m^2 W^{-1}$
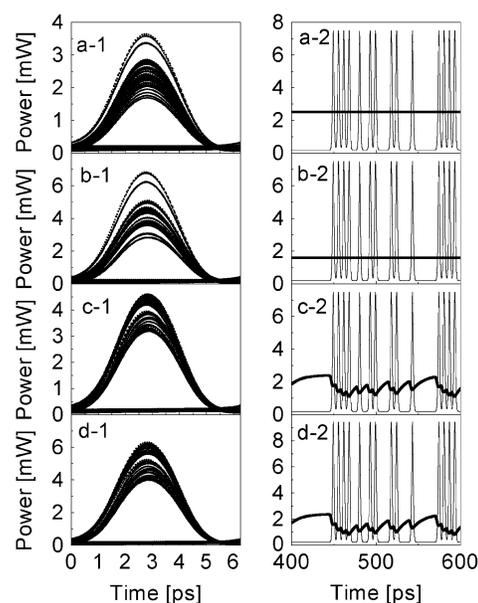
Fig. 3. 160 Gb/s noninverted wavelength converted optical eyes (left column). The input data and holding signal are shown in the right column. (a) Weak CW holding signal. (b) Strong CW holding signal. (c) XGM holding signal. (d) Increased data signal power [2 dB compared to (c)] resulting in slightly reduced average modulated holding signal power.

significantly reduced. Furthermore, the minimum mark power level is increased from 2 mW for the optimum CW holding signal to 3 mW by applying the modulated holding signal. The
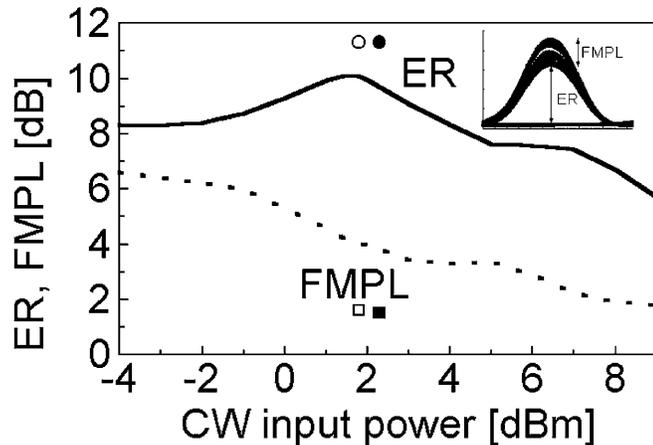
Fig. 4. Extinction ratio (ER) and fluctuations in mark power level (FMPL) in decibels as function of CW holding signal power. Other power levels and MZI operation conditions were fixed. The ER and FMPL from Fig. 3(c), (d) are indicated by solid (open) circles and squares for the ER and FMPL, respectively.
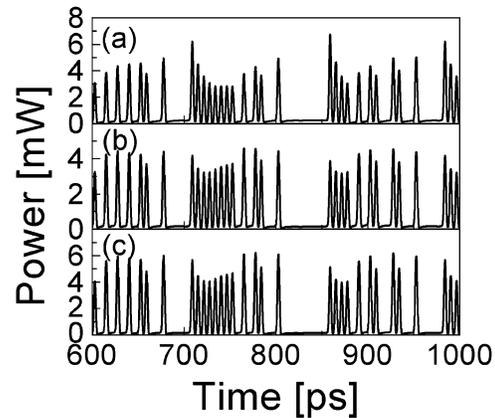

Fig. 5. Time sequence of wavelength converted signal for different holding signals. (a) is for a 2-dBm CW holding signal, while (b) and (c) are the modulated holding signals applied in Fig. 3(c) and (d), respectively.

modulated holding signal is seen to correspond to an inverted and low pass filtered version of the data signal. However, notice that the modulated holding signal is of a low quality, that does not permit retrieving the original data. The holding signals are calculated via a simple rate-equation model for an SOA, which for simplicity does not take propagation effects into account, see, e.g., [3]. Effective carrier lifetimes as low as a few tens of picoseconds have been predicted and measured for strong CW holding signals [3], [10]. The effective carrier lifetime governing the gain recovery can thus be readily modified, resulting in different temporal shapes of the modulated holding signal. The holding signals in Fig. 3(c) and (d) correspond to holding signals generated by XGM in an SOA, where the effective exponential gain recovery time $\tau_{\exp}$ was set to 12 ps.

The "grouping" of data traces in the optical eye diagrams in Fig. 3 reflect the response of the SOA to the different data sequences. Real data signals will be noisy and distorted due to amplification, fiber nonlinearities, etc., resulting in a blurring of these separate power levels. The influence of variations in the average power of the data signal has been investigated by simulating the case, where only the data signal power is increased by 2 dB, while all other parameter values were kept fixed. The resulting optical eye diagrams and modulated holding signal are shown in Fig. 3(d). It is seen that the quality of the converted signal hardly is affected, which is attributed to the inverse relation of the power of the modulated holding signal and that of the data signal. The suggested scheme should thus strongly improve the input power dynamic range.

The ER and FMPL for the converted signal in Fig. 3(c) and (d) are shown in Fig. 4 as solid and open dots and squares, respectively. The ER is increased by approximately 1.5 dB, while the FMPL is decreased by 3 dB compared to the optimum CW holding signal. We believe, however, that this is a conservative estimate of the improvements possible with this scheme. Thus, the CW holding signal was carefully optimized, while a similar detailed optimization was not performed for the modulated holding signal, due to the large numerical effort required.

The mechanism enabling a better wavelength conversion performance when using a modulated holding signal is fur-

ther elucidated in Fig. 5, where examples of the temporal characteristics of the converted signal are shown for the optimum CW case (a) and the two modulated holding signal cases, (b), (c), respectively. The eight consecutive marks in the time interval from 700–800 ps show how the converted signal intensity decreases with time and eventually becomes constant after the first 5–6 pulses in case of a CW holding signal. The modulated holding signal results in a much faster adjustment of the SOA response, such that the converted mark intensity only drops for the first three pulses, the remaining five converted pulses actually have a higher output power than the third pulse. The same feature is observed after a sequence of eight consecutive spaces, where the following mark has the highest output power in case of the CW holding signal. The maximum output mark power in case of a modulated holding signal is not observed after eight consecutive spaces, but typically after a mark space sequence. The data in Fig. 5 thus illustrate how the modulated holding signal results in a smaller pattern dependent gain modulation of the MZI SOAs after a long sequence of consecutive marks or spaces.

IV. WAVELENGTH CONVERSION AT 40 Gb/s

The influence of the shape of the modulated holding signal on the converted signal quality was also investigated by simulating wavelength conversion at a lower bit-rate of 40 Gb/s in a MZI with 500-μm-long SOAs.

The schematic of the wavelength conversion setup is shown in Fig. 2, where the wavelength converted optical eyes are illustrated for inverted as well as noninverted wavelength conversion. The MZI was in this case optimized to achieve approximately equal optical extinction ratios for inverted and noninverted wavelength conversion. Either the inverted *or* the noninverted signal could be optimized further if focusing only on one of these.

Fig. 6 shows calculated optical eye diagrams for simultaneous inverted and noninverted wavelength conversion. The simulations were performed for the set of parameter values used before (see Table I), except for the characteristics of the modulated holding signal, which are varied in order to understand, e.g., the influence of the bandwidth of the holding signal. The optical
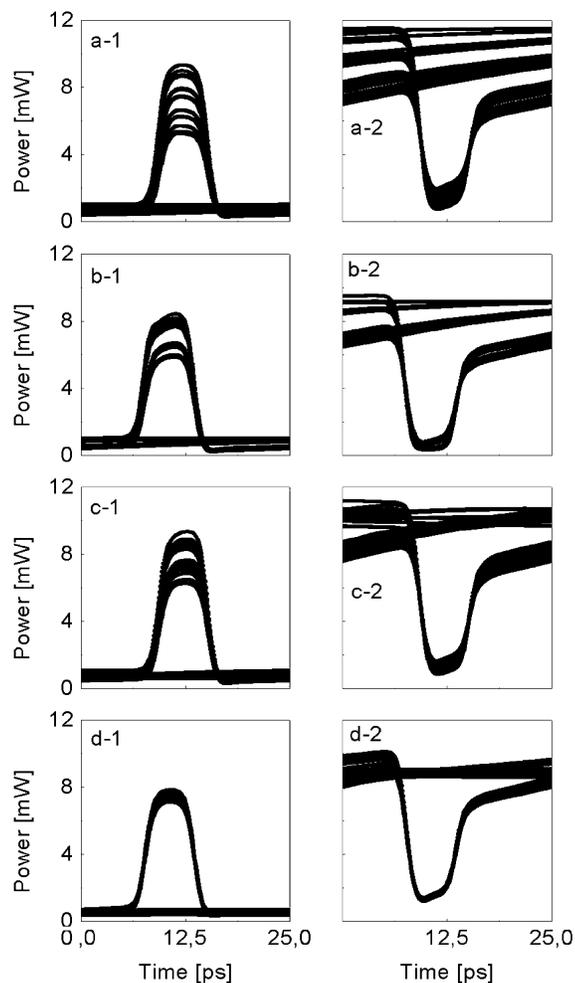
Fig. 6. Inverted and noninverted 40 Gb/s optical eye diagrams obtained using the holding signals shown in Fig. 7. The left and right column show the optical eyes in case of noninverted and inverted wavelength conversion, respectively.
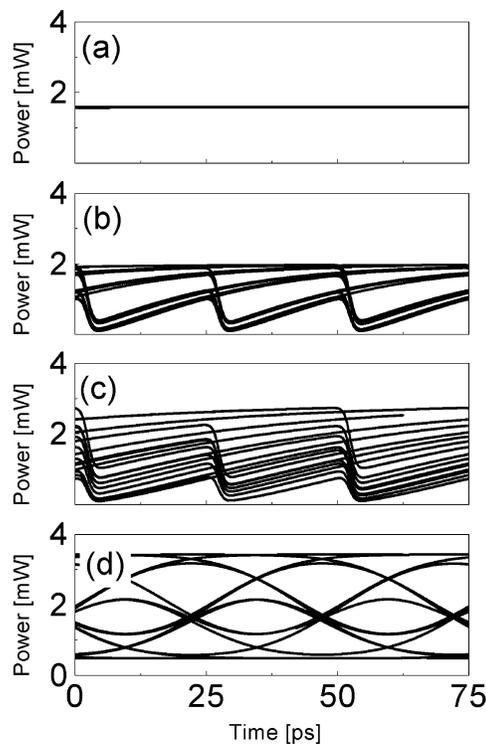

Fig. 7. Holding signals applied for the wavelength converted signals shown in Fig. 6. (a) CW holding signal. (b) XGM holding signal with $\tau_{\exp} = 20$ ps. (c) XGM holding signal with $\tau_{\exp} = 40$ ps. (d) Holding signal generated by signal inversion and low-pass filtering.

eye diagrams of the modulated holding signal corresponding to Fig. 6(a)–(d) are shown in Fig. 7(a)–(d), respectively. The simulations have again been performed using a modulated data signal similar to a PRBS signal of length $2^7 - 1$.

The optical eye diagrams in Fig. 6 show that amplitude jitter is reduced when replacing the CW holding signal Fig. 6(a) with a modulated holding signal Fig. 6(b)–(d). The jitter reduction is largest for the inverted signal, and is not simply a result of increasing the average power of the holding signal. An increased CW holding signal power would reduce the ER of the inverted optical eye and simultaneously reduce the amplitude jitter and the eye opening in the case of noninverted wavelength conversion. This is in contrast to the results shown in Fig. 6, where the optical extinction ratios for noninverted (inverted) wavelength conversion in Fig. 6(a)–(d) are 7.25 (6.62), 7.60 (9.58), 8.24 (7.55), and 10.14 dB (7.86 dB), respectively. Thus, the XGM holding signal improves the ER and reduces the amplitude jitter of the inverted and noninverted wavelength converted signal simultaneously.

In a simple p-i-n receiver model, including shot noise and thermal noise with a spectral density of $2 \cdot 10^{-22}$ A^{2}s, resulting in a back-to-back receiver sensitivity of approximately

-20 dBm for the input data signal, we find for the noninverted (inverted) wavelength converted signals in Fig. 6(a)–(d) power penalties of 3.34 (8.26), 2.84 (7.08), 2.54 (7.37), and 1.13 (7.88) dBm. The high power penalty for inverted wavelength conversion results from the short data pulses and short differential time-delay used in our setup. The average power of the inverted signal is thus significantly higher than the power in the data and noninverted data signal. The amount of thermal noise added for the back-to-back case is the same as that added for the inverted and noninverted data signal.

The power penalty calculations mainly display the improvement in ER. The reduction in amplitude jitter is poorly captured when comparing numbers like ER and power penalty. The visual comparison of the noninverted wavelength converted eyes of Fig. 6(b) and (c) shows a significantly better amplitude jitter reduction for the holding signal in Fig. 7(b), while the ER and the receiver power penalty indicate a better performance for the holding signal shown in Fig. 7(c).

The modulated holding signals shown in Figs. 7(b)–(d) have quite different temporal shapes. The holding signals in Fig. 7(b) and (c) are again calculated via the simple SOA rate-equation model, using effective exponential gain recovery times, $\tau_{\exp}$, of 20 and 40 ps for the holding signals in Fig. 7(b) and (c), respectively. The optical holding signal in Fig. 7(d) is generated by low-pass filtering the inverted data signal. This holding signal is thus somewhat artificial, but it is numerically easier to optimize the average power level and the ER in this case. The XGM holding signal in Fig. 7(d) results in a high ER and suppresses the amplitude jitter very efficiently. The holding signal has a

quite fast response with respect to adjusting its power level, depending on the bit pattern of the data signal, which is important for the suppression of amplitude jitter. On the other hand, the low-pass filtering of the signal ensures that the power of the holding signal is almost constant for a long sequence of pulses, enhancing the ER of the converted signal.

These dependencies are also observed, but less clearly, for the modulated holding signals with characteristic recovery times of 20 and 40 ps; Fig. 6(b) and (c), respectively. The fast recovery time reduces amplitude jitter, while the low pass filtering ("slower response") contributes to the enhancement of the ER.

The average power level and ER of the modulated holding signal are two other parameters, which influence the quality of the wavelength conversion. The average power level has already been considered, since the variation of the average power level results in qualitative changes similar to the case when varying the CW holding signal power level. The ER of the modulated holding signal, on the other hand describes the (maximum) variation in power. The ER of the modulated holding signal in Fig. 7(d) has been optimized for the given low-pass filtering, while the ER of the holding signals in Fig. 7(b) and (c) could be optimized further to achieve better wavelength-converted eye diagrams. However, the main limitation for the converted signals in Fig. 6(b) and (c) is the use of a single recovery time constant, which makes the generation of a holding signal similar to the holding signal in Fig. 7(d) difficult at high data rates.

The modulated holding signal is injected into both SOAs in the arms of the MZI simultaneously, as shown in Fig. 2. Introducing a variable time-delay of up to one third of the bit period between the data and the modulated holding signal hardly results in any change of the wavelength conversion performance. The timing between data and modulated holding signal is thus not critical for improving the conversion efficiency, and large timing jitter of the modulated holding signal is acceptable. It has been shown that when the data and CW signals are counter-propagating, increased timing jitter is obtained compared to the co-propagating case [11]. However, since large timing jitter is acceptable and a certain low-pass filtering of the modulated holding signal is beneficial, the generation of the modulated holding signal by counter-propagating XGM in an SOA may be preferable, since this avoids the use of an additional optical band pass filter.

V. Conclusion

We have suggested the use of a modulated holding signal to improve the performance of all-optical wavelength converters based on SOAs, in particular at high data rates. The modulated holding signal can be generated through XGM in a separate SOA. The method has been demonstrated to give a significantly better signal quality for a differentially operated MZI at 160 Gb/s, even with a low quality modulated holding signal. The generation of the holding signal would require an additional SOA or interferometer, whose bandwidth, however, does not have to match the data rate. Finally, it has been shown that the new scheme increases the robustness with respect to temporal fluctuations of the absolute data power level. The proposed scheme could thus be important to improve the performance of SOA based devices for all-optical wavelength conversion and regeneration at bit rates of 160 Gb/s and above.

References

[1] S. Nakamura, Y. Ueno, J. Sasaki, and K. Tajima, "Error-free demultiplexing at 252 Gbit/s and low-power-penalty, jitter-tolerant demultiplexing at 168 Gbit/s with integrated symmetric Mach-Zehnder all optical switch," in *ECOC'01, Proc. Eur. Conf. Opt. Comm.*, Amsterdam, The Netherlands, 2001. Paper Th.F.2.2.

[2] S. Nakamura, Y. Ueno, and K. Tajima, "168-Gb/s all-optical wavelength conversion with a symmetric-Mach-Zehnder-type switch," *IEEE Photon. Technol. Lett.*, vol. 13, pp. 1091–1093, 2001.

[3] R. J. Manning, A. D. Ellis, A. J. Poustie, and K. J. Blow, "Semiconductor laser amplifiers for ultrafast all-optical signal processing," *J. Opt. Soc. Amer. B*, vol. 14, no. 11, pp. 3204–3216, 1997.

[4] B. Dagens, A. Labrousse, S. Fabre, B. Martin, S. Squedin, B. Lavigne, R. Brenot, M. L. Nielsen, and M. Renaud, "New modular SOA-based active-passive integrated Mach-Zehnder interferometer and first standard mode 40 Gb/s all-optical wavelength conversion on the C-band," in *ECOC'02*.

[5] D. Wolfson, T. Fjelde, A. Kloch, C. Janz, A. Coquelin, I. Guillemot, F. Gaborit, F. Poingt, and M. Renaud, "Experimental investigation at 10 Gb/s of the noise suppression capabilities in a pass-through configuration in SOA-based interferometric structures," *IEEE Photon. Technol. Lett.*, vol. 7, pp. 837–839, 2000.

[6] S. Bischoff, A. Buxens, St. Fischer, M. Dülk, A. T. Clausen, H. N. Poulsen, and J. Mørk, "Comparison of all-optical co- and counter-propagating high-speed signal processing in SOA-based Mach-Zehnder interferometers," *Opt. Quantum Electron.*, vol. 33, pp. 907–926, 2001.

[7] J. Mark and J. Mørk, "Subpicosecond gain dynamics in InGaAsP optical amplifiers: Experiment and theory," *Appl. Phys. Lett.*, vol. 61, p. 2281, 1992.

[8] J. Mørk and J. Mark, "Time-resolved spectroscopy of semiconductor laser devices: Experiments and modeling," in *Proc. SPIE*, vol. 2299, 2399, 1995, pp. 146–159.

[9] A. Mecozzi and J. Mørk, "Saturation effects in nondegenerate four-wave mixing between short optical pulses in semiconductor laser amplifiers," *IEEE J. Select. Topics Quantum Electron.*, vol. 3, pp. 1190–1207, 1997.

[10] R. J. Manning and G. Sherlock, "Recovery of a π phase shift in 12.5 ps in a semiconductor laser amplifier," *IEEE Electron. Lett.*, vol. 31, pp. 307–308, 1997.

[11] A. Kloch and K. E. Stubkjaer, "Accumulation of jitter in cascaded wavelength converters based on semiconductor optical amplifiers," in *Proc. FB4 ECOC'99*, 1999.

S. Bischoff, photograph and biography not available at the time of publication.

M. L. Nielsen, photograph and biography not available at the time of publication.

J. Mørk, photograph and biography not available at the time of publication.